CIM: Constrained Intrinsic Motivation for Sparse-Reward Continuous Control

Xiang Zheng[1] , **Xingjun Ma**[2] , **Cong Wang**[1]
[1]City University of Hong Kong
[2]Fudan University
xzheng235-c@my.cityu.edu.hk, danxjma@gmail.com, congwang@cityu.edu.hk

Abstract

Intrinsic motivation is a promising exploration technique for solving reinforcement learning tasks with sparse or absent extrinsic rewards. There exist two technical challenges in implementing intrinsic motivation: 1) how to design a proper intrinsic objective to facilitate efficient exploration; and 2) how to combine the intrinsic objective with the extrinsic objective to help find better solutions. In the current literature, the intrinsic objectives are all designed in a task-agnostic manner and combined with the extrinsic objective via simple addition (or used by itself for reward-free pre-training). In this work, we show that these designs would fail in typical sparse-reward continuous control tasks. To address the problem, we propose Constrained Intrinsic Motivation (CIM) to leverage readily attainable task priors to construct a constrained intrinsic objective, and at the same time, exploit the Lagrangian method to adaptively balance the intrinsic and extrinsic objectives via a simultaneous-maximization framework. We empirically show, on multiple sparse-reward continuous control tasks, that our CIM approach achieves greatly improved performance and sample efficiency over state-of-the-art methods. Moreover, the key techniques of our CIM can also be plugged into existing methods to boost their performances.

1 Introduction

Intrinsic motivation plays an important role in exploration strategy design for sparse-reward or reward-free reinforcement learning (RL) [Barto, 2013]. It formulates the agent's familiarity with the environment as the intrinsic objective and leverages the intrinsic bonus as a measure of uncertainty to involve the agent in curiosity-driven exploration in the absence of external reward signals. Intrinsic motivation allows agents to visit novel regions more efficiently by assigning higher bonuses to unfamiliar or rarely visited states in a principled way [Liu and Abbeel, 2021b; Zhang *et al.*, 2021c]. It holds a clear advantage over heuristic dithering exploration methods that randomly disturb optimal actions regardless of the agent's learning process, e.g., Boltzman exploration or Gaussian perturbation on the policy network's parameters or outputs [Cesa-Bianchi *et al.*, 2017; Plappert *et al.*, 2017].

Intrinsic motivation has been applied in both provable and practical exploration strategies. Provable optimal exploration methods can provide sublinear bounds for sample complexity of RL algorithms in tabular and linear cases via the intrinsic Upper Confidence Bound (UCB) bonus, which captures the agent's uncertainty on estimation of the value function [He *et al.*, 2021; Zhang *et al.*, 2021d]. However, it remains challenging to efficiently compute the UCB bonus, especially in high-dimensional state space and with non-linear function approximation.

Practical exploration methods address this challenge by designing approximate intrinsic bonuses. In the current literature, there mainly exist three types of practical intrinsic motivation methods: knowledge-based, data-based, and competence-based [Laskin *et al.*, 2021]. The former two categories aim to guide the agent to cover as many states as possible when the extrinsic reward is sparse or absent [Bellemare *et al.*, 2016; Hazan *et al.*, 2019]. The last category encourages the agent to distill exploration experiences into reusable low-level skills during the exploration process [Sharma *et al.*, 2019]. Competence-based intrinsic objectives have been demonstrated to be too challenging, and agents pretrained with the competence-based intrinsic bonus even underperform those randomly initialized on downstream tasks [Laskin *et al.*, 2021].

Knowledge-based intrinsic motivation methods, in a sense analogous to the principled UCB bonus, approximate the novelty of a state in a variety of practical ways. Common approches include pseudo-count of the state visit frequency [Bellemare *et al.*, 2016; Fu *et al.*, 2017], prediction errors of a specific neural network [Pathak *et al.*, 2017; Burda *et al.*, 2018], and variances of outputs among an ensemble of neural networks [Pathak *et al.*, 2019; Lee *et al.*, 2021; Bai *et al.*, 2021b]. However, existing knowledge-based methods may suffer from problems like detachment, derailment [Ecoffet *et al.*, 2021], and catastrophic forgetting [Agarwal *et al.*, 2020a; Zhang *et al.*, 2021c]. Also, these knowledge-based intrinsic bonuses are all designed task-agnostic without considering any available task priors. What's more, knowledge-based intrinsic bonuses are usually trivially added to the extrinsic reward, which can introduce bias to the extrinsic objective [Zhang *et al.*, 2021c].

Data-based intrinsic motivation is simple yet promising for solving sparse-reward RL tasks among the above three practical intrinsic motivation categories. It achieves state coverage by maximizing the state entropy [Hazan *et al.*, 2019]. Recently, the non-parametric k-nearest neighbor (k-NN) estimator has been utilized for efficient state entropy estimation for either state-based [Mutti *et al.*, 2021] or pixel-based RL tasks [Liu and Abbeel, 2021a; Liu and Abbeel, 2021b; Seo *et al.*, 2021]. However, these methods either aim only for reward-free pure exploration [Hazan *et al.*, 2019] or adopt the reward-free pre-training paradigm to solve downstream RL tasks [Liu and Abbeel, 2021b; Seo *et al.*, 2021]. Laskin [2021] demonstrated that these training paradigms are inefficient in both state-based and pixel-based sparse-reward RL tasks. Though Seo [2021] also considers online RL tasks, their method depends on the random encoder's visual inductive bias and thus is only suitable for pixel-based RL. Furthermore, these data-based methods also task-agnostically design their intrinsic objectives and bonuses, as summarized in Table 2. This design is ineffective in various sparse-reward continuous control tasks as we will show in the experiments.

Motivated by the above limitations of existing approaches, in this work we propose Constrained Intrinsic Motivation (CIM) for efficient exploration in sparse-reward RL by 1) constructing a proper constrained intrinsic motivation via attainable high-level task priors, and 2) adaptively adjusting the strength of intrinsic motivation according to the learning progress of the agent.

In summary, we make the following contributions:

- We propose Constrained Intrinsic Motivation (CIM), which overcomes the limitation of the current task-agnostic design principle and inefficient combining methods for intrinsic motivation. CIM outperforms state-of-the-art intrinsic motivation methods with greatly improved performance and sample efficiency on various sparse-reward continuous control tasks.
- CIM formulates the attainable high-level task prior as a general composite projector, and designs the constrained intrinsic objective and bonus in the low-dimensional projection space. This design is able to intrinsically encourage the agent to explore only task-related regions without hand-craft rewards. CIM presents a novel approach for integrating task priors into RL to improve sample- and compute-efficiency.
- CIM formulates the simultaneous-maximization problem of the intrinsic and extrinsic objectives as a convex Markov Decision Process (MDP) and solves the constrained optimization problem via the Lagrangian method with adaptively updated constraint (based on the agent's learning progress). We demonstrate that the Lagrangian method can effectively diminish the bias introduced by the intrinsic motivation.
- We also show that the two novel techniques used in our CIM, the task-prior projector and the Lagrangian method, can be easily plugged into existing knowledge-based and data-based exploration methods to help boost their performances.

2 Preliminaries

2.1 Intrinsically Motivated RL

In RL tasks, the agent interacts with the environment sequentially and aims to learn an optimal policy that maximizes the expected cumulative extrinsic reward specified by the task. The interactions are often defined using discounted MDP $M = (\mathcal{S}, \mathcal{A}, P, R, \gamma, \mu)$, where $\mathcal{S}$ and $\mathcal{A}$ stand for state space and action space separately, $P : \mathcal{S} \times \mathcal{A} \to \Delta(\mathcal{S})$ is a transition funtion mapping state s and action a to $P(s'|s, a)$ in the space of probability distribution $\Delta(\mathcal{S})$ over S, $R : \mathcal{S} \times \mathcal{A} \times \mathcal{S} \to \mathbb{R}$ is the reward function and usually assumed te be bounded, $\gamma \in [0, 1)$ is the discount factor which determines the horizon for the problem, and $\mu \in \Delta(\mathcal{S})$ is the initial state distribution. We focus on episodic MDP. At the beginning of each episode, the agent samples a random initial state $s_0 \sim \mu$; at each time $t = 0, 1, 2, ...$, it takes an action $a_t \in \mathcal{A}$ computed by a stochastic policy $\pi : \mathcal{S} \to \Delta(\mathcal{A})$ or a deterministic one $\pi : \mathcal{S} \to \mathcal{A}$ according to the current state s_t and steps into the next state $s_{t+1} \sim P(\cdot|s_t, a_t)$ with an instant reward signal $r_t = R(s_t, a_t, s_{t+1})$ obtained. The episode is reset once the finite horizon is reached or the task is completed or failed.

In intrinsically motivated exploration methods, there are two types of reward functions, including the extrinsic reward function $r^e := R_e(s, a, s')$ and the intrinsic one $r^i := R_i(s, a, s')$. To introduce the formal intrinsic objective, we first define the $t-$step state distribution and the (discounted) state distribution induced by a policy π as

$$\begin{aligned} d_{t,\pi}(s, a) &= P\left(s_t = s, a_t = a \mid \pi\right) \\ &= \sum_{\substack{\text{all } \tau \text{ with} \\ s_t = s, a_t = a}} P(\tau \mid \pi) \end{aligned} \tag{1}$$

$$d_\pi(s) = (1 - \gamma) \sum_{t=1}^{\infty} \gamma^t \sum_a d_{t,\pi}(s, a) \tag{2}$$

where $\tau = (s_0, a_0, s_1, a_1, \cdots)$ is the trajectory [Hazan *et al.*, 2019]. The common extrinsic reward maximization problem is then derived as

$$\max_{d_\pi \in \mathcal{K}} \mathop{\mathbb{E}}_{s \sim d_\pi} r^e \tag{3}$$

where $\mathcal{K}$ is the collection of all induced distributions d_π. A common definition of r^e in sparse-reward RL tasks is

$$r^e = \begin{cases} 1, & \text{if } \mathrm{proj}_{\mathcal{P}}\, s' \in \mathcal{G} \\ 0, & \text{otherwise} \end{cases} \tag{4}$$

where $\mathcal{P}$ is a projection space (e.g., a 2D map), which is a subspace of the full state space, $\mathrm{proj}_{\mathcal{P}}$ is a projection operator mapping state s' from $\mathcal{S}$ to $\mathcal{P}$, and $\mathcal{G}$ is the goal space where all desired task goals are located (e.g., all target locations in the 2D map).

In convex MDP, the intrinsic objective is defined as a differentiable function $f_i : \mathcal{K} \to \mathbb{R}$ of the induced state distribution d_π with $L-$Lipschitz gradient. The common unconstrained optimization objective by simply summing the intrinsic objective and the extrinsic objective is then

$$\max_{d_\pi \in \mathcal{K}} f_e(d_\pi) + \lambda f_i(d_\pi) \tag{5}$$

where $f_e(d_\pi) := \mathbb{E}_{s\sim d_\pi} r^e$ is the extrinsic objective as defined in Equation (3), and λ is a constant coefficient to balance the two objectives. Common choices of f_i include the differential entropy of the induced state distribution

$$f_i(d_\pi) = \mathop{\mathbb{E}}_{s\sim d_\pi} [-\ln d_\pi(s)] \tag{6}$$

to expect the induced state distribution to be as uniform as possible, and the negative reverse Kullback–Leibler (KL) divergence between d_π and a target state distribution Q

$$f_i(d_\pi) = \mathop{\mathbb{E}}_{s\sim d_\pi} [-\ln d_\pi(s) + \ln q(s)] \tag{7}$$

to let d_π seek a certain mode of Q where $q(s)$ denote the probability density of Q [Hazan *et al.*, 2019]. The regularizer used in the state-of-the-art exploration method MAximizes the DEviation (MADE) [Zhang *et al.*, 2021c] can be recovered by defining

$$f_i(d_\pi) = \mathop{\mathbb{E}}_{s\sim d_\pi} \sqrt{\rho_{\text{cov},l}^{-1} d_\pi} \tag{8}$$

where $\rho_{\text{cov},l} = \frac{1}{l}\sum_{i=1}^{l} d_{\pi_i}$ is the policy coverage induced by the uniform mixture of all past policies at the l^{th} iteration of the training process.

2.2 Differential Entropy Estimator

Instead of training a parametric generative model to estimate the state density d_π, we leverage a more practical non-parametric $k-$nearest neighbor ($k-$NN) differential entropy estimator. Recall the differential entropy of a random variable X is defined as

$$h(X) = -\int_{\mathcal{X}} f(x)\ln f(x) dx \tag{9}$$

where $f(x)$ is the probability density function and $\mathcal{X}$ is the support set of $X \subset \mathbb{R}^d$. Suppose we sample n independent identically distributed (i.i.d.) random vectors $\mathbf{X} = \{X_1, \ldots, X_n\}$ from f, we can estimate the differential entropy by

$$h(f) \approx \frac{1}{n}\sum_{i=1}^{n} -\ln \hat{f}\left(X_i\right) \tag{10}$$

where

$$\hat{f}\left(X_i\right) = \frac{\int_{B(X_i,R_{i,k})} f(u)\mathrm{d}u}{\lambda\left(B\left(X_i, R_{i,k}\right)\right)} \approx \frac{k}{n\lambda\left(B\right)} \tag{11}$$

is the average density of the neighborhood B near X_i, λ is the Lebesgue measure on $\mathbb{R}^d$, $R_{i,k} = \|X_i - X_i^{k-\text{NN}}\|$ is the distance between X_i and its k^{th}-nearest neighbor $X_i^{k-\text{NN}} \in \mathbf{X}\setminus\{X_i\}$.

Lemma 1 ([Jiao *et al.*, 2018])**.** *The k-nearest neighbor entropy estimator for $h(f)$*

$$\hat{h}_{n,k}(\mathbf{X}) = \frac{1}{n}\sum_{i=1}^{n} \ln\left(\frac{n}{k}\lambda\left(B\left(X_i, R_{i,k}\right)\right)\right) + b$$

is adaptively near minimax rate-optimal, where $b = \ln k - \psi(k)$ is a constant bias term, $\psi(k)$ is the digamma function.

3 Constrained Intrinsic Motivation

In this section, we present the overall design of the proposed Constrained Intrinsic Motivation (CIM) for efficient exploration in sparse-reward RL. CIM constrains intrinsic motivation from two aspects. First, we leverage the attainable high-level task priors that commonly exist in sparse-reward continuous control tasks to constrain the intrinsic bonuses, i.e., by limiting them to be only effective in the task-related projection space. An example is illustrated in Figure 1a. Secondly, we use the Lagrangian method to adaptively balance the intrinsic and extrinsic objectives when simultaneously maximizing the two.

3.1 Constraining Intrinsic Motivation via Prior

Current intrinsic motivation exploration methods become less efficient when the state space is large. To address this issue, we leverage the high-level task priors to define a projection space $\mathcal{P}$ to constrain the exploration region and design constrained intrinsic objective via a task-prior projector. Specifically, we maximize the entropy of the projected (instead of the full or latent) state distribution. The space where the state entropy is estimated is critical for the agent's learning process. When the full state space is sophisticated, entropies of the state distribution estimated in different dimensions can be conflicting, e.g., the diversity of the acceleration does not imply the diversity of the position. Estimating the state entropy in the latent space cannot alleviate this problem. The projection space might not be embedded in the state space. However, when the state is assumed to be fully observable, we can always expand the state space $\tilde{\mathcal{S}} = \mathcal{S}\cup\mathcal{P}$ to make the projection space a subspace of the state space. We thus focus on the setting $\mathcal{P}\subset\mathcal{S}$.

Task-prior Projector

In general, the projection space can be an arbitrary topological space. For simplicity, we formulate task-prior projectors as the following without loss of generality

$$\text{proj}_{\mathcal{P}} := m^p \odot \left[e_{i_1}\, e_{i_2} \cdots e_{i_m}\right]^\intercal \tag{12}$$

where the masking operator

$$m^p = [f_1(s_{i_1}), f_2(s_{i_2}), \ldots, f_m(s_{i_m})]^\intercal \tag{13}$$

is a $m\times 1$ vector-valued function determined by the task prior to constrain the task-related region in the projection space, e_{i_j} is the basis vector of space $\mathcal{S}$ with the i_j-th element is 1 and others 0, i_j is the index of the dimension implied by the task prior, $j = 1, 2, ..., m$. Each part of this composite operator is related to the task prior, distinguished from the task-agnostic projection space definition in MaxEnt and MEPOL. For instance, m^p in SAnt can be defined as $[\mathbb{1}[x > 0], \mathbb{1}[v_x > 0]]$, as shown in Figure 1a. This kind of task priors commonly exists and is attainable in control tasks like SAnt.

Besides having the advantage of constraining the exploration region implied by the high-level task prior, estimating the state entropy in the projection space is also advantageous in computational efficiency, considering that the computational complexity of the $k-$nearest neighbors algorithm is $\mathcal{O}(mn\ln(n))$. For instance, the default dimension of the

Table 1: Comparing methods of knowledge-based and data-based intrinsic motivation for sparse-reward RL, including ICM, RND, MADE, MaxEnt, MEPOL, RE3, APT, among which MADE and APT are SOTA methods. **Intrinsic Objective**: heuristic intrinsic motivation (e.g. sparsity as novelty in ICM) or theoretical intrinsic optimization objective (e.g. the differential entropy of the state distribution in MaxEnt, or the policy-coverage-based regulator in MADE). **Intrinsic Bonus**: intrinsic bonuses parametrically (e.g. MADE) or nonparametrically (e.g. APT) approximated. **Intrinsic Input Space**: state space where the intrinsic objective or bonus is designed (full or latent or projected state space). **Combining Method** categorizes how intrinsic and extrinsic objectives are combined: simple addition (e.g. ICM), using only intrinsic objective (e.g. MaxEnt), separating them clearly in different training phases (e.g. APT), or adaptively balancing the two as in our CIM. Extended related work on exploration methods for sparse-reward RL can be found in Appendix A.

Method	Intrinsic Objective	Intrinsic Bonus	Intrinsic Input Space	Combining Method
ICM	$\mathbb{E}_{s\sim d_\pi}\rho_{\text{cov},l}^{-1}$	$\|f^{\text{ICM}}(\phi(s_t),a_t)-\phi(s_{t+1})\|$	Learned Latent	$\lambda r_t^i + r_t^e$
RND	$\mathbb{E}_{s\sim d_\pi}\rho_{\text{cov},l}^{-1}$	$\|f^{\text{RND}}(\phi(s_t))-f^*(\phi(s_t))\|$	Learned Latent/Full	$\lambda r_t^i + r_t^e$
MADE	$\mathbb{E}_{s\sim d_\pi}\sqrt{\rho_{\text{cov},l}^{-1}d_\pi^{-1}}$	$\sqrt{r_t^{\text{RND}}r_t^{\text{VAE}}}$	Learned Latent/Full	$\lambda r_t^i + r_t^e$
MaxEnt	$\mathbb{E}_{s\sim d_\pi}[-\ln d_\pi(s)]$	$-\ln \hat{d}_\pi(s)$	Task-agnostic Projection	r_t^i
MEPOL	$\mathbb{E}_{s\sim d_\pi}[-\ln d_\pi(s)]$	None	Task-agnostic Projection	$\mathbb{1}[t\le N]r_t^i + \mathbb{1}[t>N]r_t^e$
RE3	$\mathbb{E}_{s\sim d_\pi}[-\ln d_\pi(s)]$	$\ln(1+R_{t,k}^l)$	Random Latent	$\mathbb{1}[t\le N]r_t^i + \mathbb{1}[t>N]r_t^e$
APT	$\mathbb{E}_{s\sim d_\pi}[-\ln d_\pi(s)]$	$\ln(1+R_{t,k}^{l/f})$	Learned Latent/Full	$\mathbb{1}[t\le N]r_t^i + \mathbb{1}[t>N]r_t^e$
CIM (ours)	$\mathbb{E}_{s\sim d_\pi}[-\ln \boldsymbol{d_\pi^p}(s)]$	$\ln(1+\boldsymbol{R_{t,k}^p})$	**Task-prior Projection**	$\max(\boldsymbol{\lambda_l},1)^{-1}r_t^i + r_t^e$

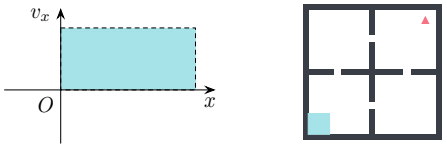

(a)

(b)

Figure 1: (a) A two-dimensional quarter projection space used in the MuJoCo sparse-reward continuous control task SparseAnt-x10-v0 (SAnt). (b) Four-room layout of the classic continuous control task SparseGridWorld-v0. The blue square is the starting region of the agent, the red triangular is the target location, and the black lines are the walls.

latent space in APT is 1024 in their original paper, the dimension of the full state of a Humanoid is 376, while the dimension of the projection space in our CIM is only 2.

Constrained Intrinsic Objective

With the definition of the task-prior projector, we now introduce the constrained intrinsic objective used in CIM. We define the (discounted) projected state distribution induced by a policy π as

$$d_{t,\pi}^p(s,a) = P\left(\text{proj}_{\mathcal{P}}\, s_t = \text{proj}_{\mathcal{P}}\, s, a_t = a \mid \pi\right) \tag{14}$$

$$d_\pi^p(s) = (1-\gamma)\sum_{t=1}^{\infty}\gamma^t \sum_a d_{t,\pi}^p(s,a) \tag{15}$$

Our principled intrinsic objective constrained by task priors is then

$$f_i^{\text{CIM}}(d_\pi^p) = \mathop{\mathbb{E}}_{\text{proj}_{\mathcal{P}}\, s\sim d_\pi^p}[-\ln d_\pi^p(s)] \tag{16}$$

which is the entropy of the projected state distribution.

Theorem 2. *Given $\mathcal{P}\subset\mathcal{S}$, the entropy of the projecetd state distribution can be estimated as*

$$\hat{h}_{n,k}^p(\mathbf{S}) = \frac{m}{n}\sum_{i=1}^{n}\ln\left(R_{i,k}^p\right) + b$$

where $\mathbf{S}=\{s_1,s_2,...,s_n\}$ is a collection of n i.i.d. state samples, m is the dimension of the projection space, $R_{i,k}^p = \|x_i - (x_i)^{k-NN}\|$ is the distance between the projected state $x_i := \text{proj}_{\mathcal{P}}\, s_i$ and its k^{th}-nearest neighbor $(x_i)^{k-NN}\in\{x_j\}_{j=1,j\neq i}^n$, b is the correction term.

Proof. Note that the average density of the neighborhood near x_i is

$$\hat{f}^p(x_i) \approx \frac{k}{n\lambda\left(B\left(x_i, R_{i,k}^p\right)\right)} = \frac{k}{n}\left(R_{i,k}^p\right)^{-m}. \tag{17}$$

According to Lemma 1, Theorem 2 can be verified. □

Remark. Theorem 2 tells us that $\hat{f}^p(x_i)$ is a good nonparametric approximator for $d_\pi^p(s)$.

Intrinsic Bonus Design

When using a differentiable intrinsic objective $f_i(d_\pi)$ that is concave in the state distribution space $\mathcal{K}$ like the (projected) state entropy, the intrinsic reward function can be defined as follows according to Lemma 4

$$r_t^i := (\nabla f_i(d_\pi))_{s_t} = \left(\frac{\mathrm{d}f_i}{\mathrm{d}d_\pi}\right)_{s_t} \tag{18}$$

where $\nabla f_i(d_\pi)$ can be regarded as an infinite column vector of which each element is a reward r_t^i at state s_t. It can be verified that $r^e = \nabla f_e(d_\pi)$, which recovers the extrinsic reward function.

Lemma 3 ([Puterman, 2014])**.** *Given the set of all induced distribution $\mathcal{K}$, for any d, the following equation holds*

$$\sum_a d(s', a) = (1-\gamma)\mu + \gamma \sum_{s,a} P(s' \mid s, a) d(s, a).$$

Lemma 4 ([Hazan *et al.*, 2019])**.** *Given any differentiable intrinsic objective f_i with L-Lipschitz gradient and the intrinsic reward function defined as Equation (18), there exists an oracle-efficient algorithm such that for any sub-optimality gap $\varepsilon > 0$, it returns a policy π with the guarantee that $f_i(d_\pi) > max_{\pi \in \pi} f_i(d_\pi) - \varepsilon$.*

Remark. Lemma 4 can be proved using the Frank-Wolfe Algorithm, a first-order method for nonlinear constrained optimization. According to Lemma 3, $\mathcal{K}$ is a convex and compact set and for any $d \in \mathcal{K}$, there exists a policy π of which the induced state distribution holds $d_\pi = d$. The core insight is to search in the state distribution space $\mathcal{K}$ instead of the policy space π. The Frank-Wolfe gap at the l^{th} iteration for the intrinsic objective f_i is then

$$g_l(d) = \langle \nabla f_i(d_{\pi_l}), d_{\pi_l} - d \rangle$$

The induced state distribution that maximizes the intrinsic objective f_i can then be reached in a recursive way

$$d_{\pi_{l+1}} = (1-\eta) d_{\pi_l} + \eta d_l$$

where $d_l \in \arg\min_{d \in \mathcal{K}} g_l$ and η is the step size of updating. d_l can be solved by any state-of-the-art planning oracle which can return a near-optimal policy under any reward function.

It is easy to verify that d_π^p also obeys Lemma 3 and Lemma 4. Note that $\nabla h(P)_i = -\ln(P_i) - 1$ where $P \in \mathcal{K}$ [Hazan *et al.*, 2019], according to Equation (16)-(18), our intrinsic bonus can be derived as

$$r_t^{\text{CIM}} = -\ln \hat{f}^p(x_t) - 1 \propto \ln R_{t,k}^p \tag{19}$$

To make the learning process more stable, we use the following "average" version

$$r_t^{\text{CIM}} = \ln \left(1 + \frac{1}{k} \sum_{i=1}^{k} R_{t,i}^p \right) \tag{20}$$

3.2 Constraining Intrinsic Motivation via Lagrangian

In this section, we introduce our novel Lagrangian-based method for exploration with intrinsic motivation. Though maximizing the (projected) state entropy objective can encourage the agent to explore larger regions, it suffers from the inconsistency problem; the intrinsic reward does not converge to zero and introduces unvanished bias into the convergent policy. We solve this challenging problem by formulating it as a reward-constrained convex MDP. Specifically, CIM reformulates Equation (5) as follows by taking the maximization of the extrinsic objective as a constraint

$$\begin{aligned} &\max_{d_\pi \in \mathcal{K}} f_i(d_\pi) \\ &\text{s.t. } f_e(d_\pi) \geq \hat{R} \end{aligned} \tag{21}$$

where $\hat{R}$ is the expected reward. This formulation provides a novel perspective for combining intrinsic and extrinsic objectives.

Small $\hat{R}$ makes it possible for the agent to focus on the intrinsic objective $f_i(d_\pi)$ in the early learning phase. By adaptively increasing the expected reward $\hat{R}$ according to the performance of the agent, it can turn to focus on the extrinsic objective $f_e(d_\pi)$ in the later learning phase. Specifically, We design a heuristic scheduler for $\hat{R}$

$$\hat{R}_l = \alpha f_e(d_{\pi_{l-1}}), \alpha > 1 \tag{22}$$

which can be viewed as an automated curriculum to adjust the strength of the constraint according to the current performance of the agent. In the early learning stage, the constraint is always satisfied, observing that $\hat{R}_l$ and $f_e(d_{\pi_l})$ are both zero, which means the agent concentrates upon the maximization of the intrinsic objective $f_i(d_\pi)$. Once $f_e(d_{\pi_l})$ becomes non-zero, $\hat{R}_l$ automatically start to grow.

Lagrangian Method

To solve Equation (21), we leverage the Lagrangian method. The Lagrangian of Equation (21) is

$$\mathcal{L}(d_\pi, \lambda) = f_i(d_\pi) + \lambda (f_e(d_\pi) - \hat{R}) \tag{23}$$

where the second term $\lambda(f_e(d_\pi) - \hat{R})$ serves as the upper bound of $-\infty$ when $f_e(d_\pi) < \hat{R}$. The corresponding Lagrangian dual problem of Equation (21) is

$$\min_{\lambda \geq 0} \max_{d_\pi} \mathcal{L}(d_\pi, \lambda) \tag{24}$$

where λ is the Lagrangian multiplier that provides an adaptive way to balance the intrinsic and extrinsic objectives. λ can be updated by gradient descent

$$\lambda_{l+1} = \lambda_l - \eta_l (f_e(d_{\pi_l}) - \hat{R}_l) \tag{25}$$

where η_l is the step size of updating at the l^{th} iteration. To make the learning process more stable, we use the following equal form of Equation (23)

$$\tilde{\mathcal{L}}_l(d_\pi, \lambda) = \tilde{\lambda}_l^{-1} f_i(d_\pi) + (f_e(d_\pi) - \hat{R}_l) \tag{26}$$

where $\tilde{\lambda}_l = \max(\lambda_l, 1)$. As $f_e(d_{\pi_l})$ increases, $\tilde{\lambda}_l$ decreases gradually towards zero.

Relationship with Other Combining Methods

The Lagrangian method provides a unified view for all combining methods listed in Tabel 2. For instance, the reward-free pre-training method can be recovered by setting $\hat{R}_l = \mathbb{1}[l > N]$, $\lambda_0 = 0$, and $\eta_l = +\infty$, where N is the total pre-training steps. And the simple addition based combining method can be derived by setting $\hat{R}_l = 0$, $\lambda_0 = \lambda_p$, and $\eta_l = 0$.

4 Experiments

4.1 Experimental Setup

We evaluate our CIM in a variety of widely-used sparse-reward continuous control environments, including two classic control tasks and three MuJoCo control tasks. Appendix

B contains more details about these environments. We select the state-of-the-art on-policy RL Proximal Policy Optimization (PPO) [Schulman *et al.*, 2017] as the policy learning oracle and implement it based on Tianshou [Weng *et al.*, 2021]. Note that our CIM is also suitable for off-policy RL. We leave CIM with off-policy RL for future work. Hyperparameters of PPO are kept the same for all experiments, and each configuration is evaluated with 5 seeds. The oracle PPO with only the extrinsic sparse reward defined by Equation (4) fails to learn all these challenging tasks. Hence, we omit this weak baseline in all figures to make them concise. We use KeOps [Feydy *et al.*, 2020] to compute $k-$NN distances. More details about the algorithm and implementation of our CIM can be found in Appendix C.

Baselines

We implement various state-of-the-art intrinsic bonuses as our baselines, including ICM [Pathak *et al.*, 2017], RND [Burda *et al.*, 2018], APT [Liu and Abbeel, 2021b], and MADE [Zhang *et al.*, 2021c]. We do not consider MaxEnt [Hazan *et al.*, 2019] which is designed only for reward-free pure exploration, MEPOL [Mutti *et al.*, 2021] which does not use intrinsic bonus, and RE3 [Seo *et al.*, 2021] which is only suitable for pixel-based RL, as summarized in Table 2. ICM and RND use the prediction error of neural networks to represent the novelty. ICM uses a forward dynamic predictor while RND trains one neural network to predict the output of another fixed randomly initialized neural network. The bonus of MADE is the geometric average of the RND bonus and the prediction error of an autoencoder, which is only trained with the current batch of samples and is reinitialized at the beginning of each epoch to approximate the weighted mixture of the induced state distribution. APT adopts a nonparametrically approximated bonus similar to our CIM bonus. The main difference between the APT and CIM bonuses is that APT approximates the bonus in the full state or a learned latent state space, while our CIM approximates the bonus in the projection space determined by high-level task priors. Moreover, the APT bonus is only evaluated in the reward-free pre-training paradigm in their original paper. We empirically demonstrate the inefficiency of both the APT bonus and the reward-free pre-training paradigm on various sparse-reward continuous control tasks. For more implementation details of the baselines, please refer to Appendix C.3.

4.2 Classic Control Tasks

Task Description

We first select two classic control tasks, SparseGridWorld-v0 (SGridWorld, 2-D) and SparsePendulum-v0 (SPendulum, 3-D), as toy environments to investigate the efficiency of different intrinsic bonuses and different combining methods. Figure 1b shows the map of SparseGridWorld-v0. The area of the map is 12m$\times$12m, and the radius of the target region is 0.1m. SparsePendulum-v0 is the gym PendulumEnv swinging a pendulum from bottom to top with a custom sparse reward that is only nonzero within extremely small error thresholds of both angular position (1deg) and velocity (1deg/sec) at the highest location. Note that the projection space is the same as the full space in these two low-dimensional tasks

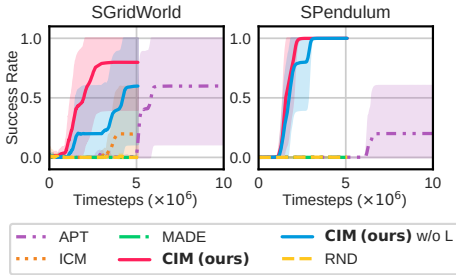

Figure 2: Performance on classic control tasks. CIM outperforms all baselines in the two low-dimensional tasks. Both RND and MADE failed the two tasks.

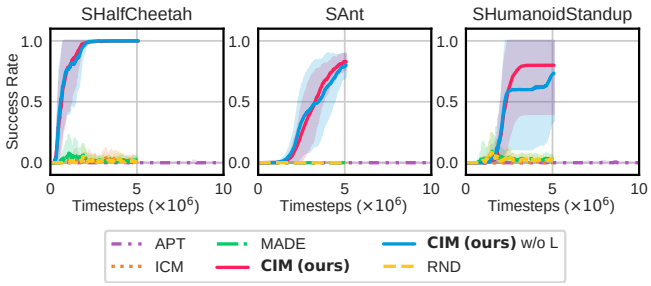

Figure 3: Performance on MoJoCo control tasks. CIM significantly surpasses all baselines in these three high-dimensional tasks. Only our CIM can consistently solve all tasks.

CIM Outperforms All Baselines in Low-Dimensional Tasks

Figure 2 shows that our CIM surpasses all baseline methods consistently in both tasks, reaching a mean success rate of 0.8 and 1 in SGridWorld and SPendulum, respectively. The low performance of APT in SPendulum reveals the ineffective transferability of the reward-free pre-trained policy. The success rate of ICM is low in SGidWorld and nearly zero in SPendulum, and RND and MADE even failed both tasks. This show the instability of these knownledge-based intrinsic motivation methods.

Effect of Lagrangian (L)

As shown in Figure 2, the ablation study on the Lagrangian method (CIM v.s. CIM w/o L) reveals that it can effectively balance the intrinsic and extrinsic objectives. The Lagrangian method can successfully reduces the bias introduced by the intrinsic motivation so that the agent is less distracted by the intrinsic motivation after it reaches the target location for the first time.

4.3 MuJoCo Control Tasks

Task Description

We select three high-dimensional MuJoCo control tasks, including SparseHalfCheetah-x20-v0 (SHalfCheetah, 18-D), SparseAnt-x10-v0 (SAnt, 113-D), and SparseHumanoidStandup-z1-v0 (SHumanoidStandup, 376-D), where x10 in SparseAnt-x10-v0 means that the Ant can only get extrinsic rewards when it can run more than 10 meters along the positive direction of the x axis. The meanings of x20 and z1 are similar.

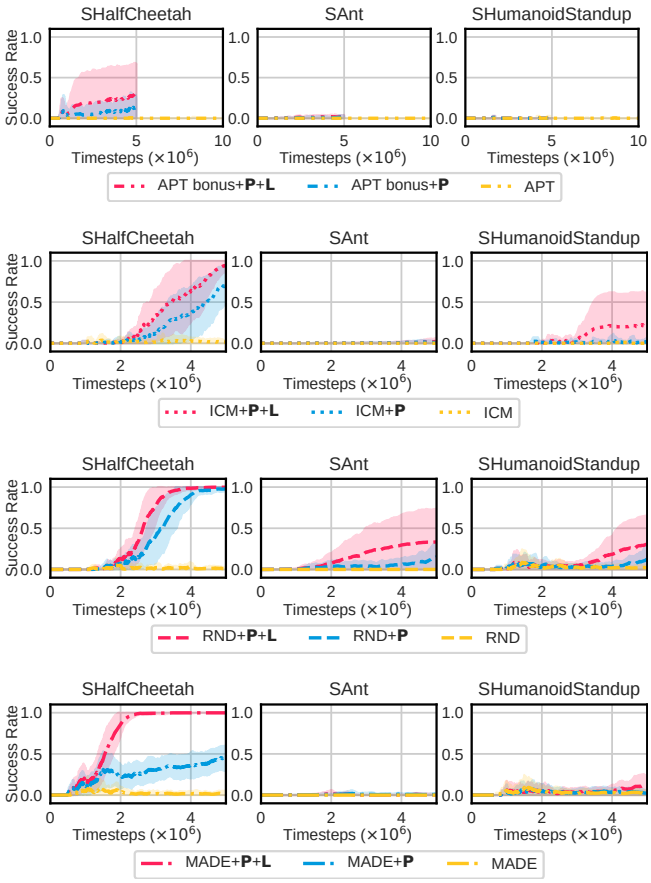

Figure 4: Plug-in study on MuJoCo control tasks. Performances of all baseline intrinsic bonuses, including APT, ICM, RND, and MADE, can be boosted reasonably via Prior (P) and Lagrangian (L), especially in SHalfCheetah.

CIM Greatly Outperforms All Baselines in High-Dimensional Tasks

The advantage of our CIM is more pronouced in the more challegning high-dimensional tasks, as shown in Figure 3. Note that APT successfully solves the two low-dimensional tasks yet fails all the three high-dimensional tasks. This indicates that the task-prior projector used in our CIM can effectively tackle the high-dimensional challenge. What's more, the ablation study on the Lagrangian method (CIM v.s. CIM w/o L) again shows that the Lagrangian method used in CIM contributes substantially to the entire learning process. More detailed analysis can be found in Appendix D.

Effect of Prior (P) and Lagrangian (L)

We conduct comprehensive experiments to further demonstrate the advantages of the two key technqiues used in our CIM, i.e., the task-prior projector and the Lagrangian method. We plug the two technqiues independetnly into knowledge-based and data-based intrinsic bonuses to improve existing methods. For the intrinsic bonus whose input space is the full state space or the latent space, we use the masking function $\tilde{m}(s) := \mathbb{1}[\det(\mathrm{diag}(m^p)) = 1]$. Figure 4 shows that both the task-prior masking function and the Lagrangian method can boost the performance of these baseline bonuses in SHalfCheetah. Specifically, the task-prior masking function effectively prevents the agent from exploring task-irrelevant space. The effect of the task-prior masking function is more evident for knowledge-based bonuses (e.g. RND+P) than data-based one (APT bonus+P). One reason of this difference is probably that the estimation inaccuracy of the latent state entropy is amplified in these high-dimensional tasks. The Lagrangian method can further boost the performance of the masked bonuses (especially MADE+P+L by nearly half) by reducing the bias introduced by the intrinsic motivation. It is also reasonable that when the task-prior masking cannot ameliorate the sample efficiency of the intrinsic bonus (e.g. ICM+P in SAnt), Lagrangian as a balance method also cannot take effect due to the agent's poor exploration ability.

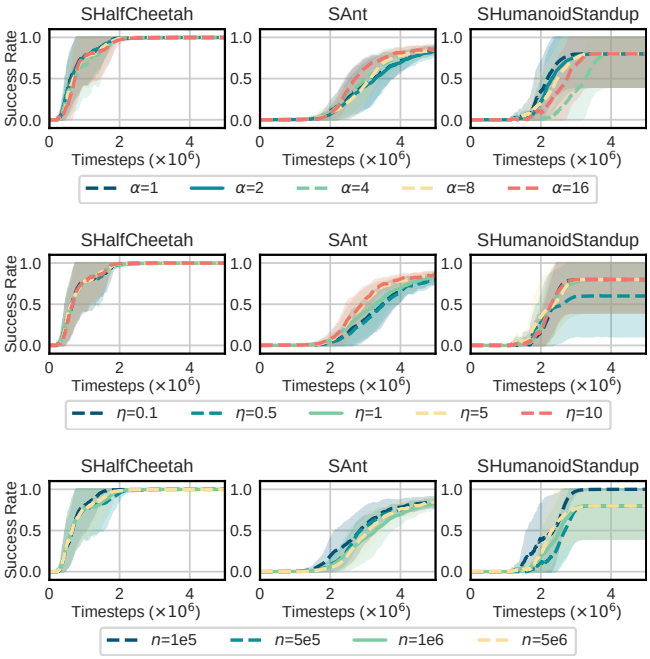

Figure 5: Ablation study on MuJoCo control tasks. The expected reward schedule's growth rate α, the Lagrangian coefficient's update step size η, and the sample size n for the entropy estimator are all robust across a large range. The solid line is the default setting.

Ablation Study

Here we test the sensitivity of our CIM to its newly introduced hyperparameters. The results are visualized in Figure 5 where it shows that CIM is insensitive to all hyperparameters. In fact, the performance of our CIM is rather stable across a quite large range of hyperparameter settings. More ablation study can be found in Appendix E.

5 Conclusion

In this paper, we proposed Constrained Intrinsic Motivation (CIM), a simple yet efficient exploration method for sparse-reward RL. CIM effectively constrains the intrinsic motivation by integrating attainable task priors into the intrinsic state entropy bonuses so as to encourage the agent to cover more

task-related regions. Meanwhile, CIM adaptively balances intrinsic and extrinsic objectives via the Lagrangian method. Our results demonstrate that both techniques are essential for CIM to solve various challenging sparse-reward continuous control tasks. We emphasize that our goal is not to find the best task prior for a specific task, but to present a novel design principle for intrinsic motivaiton. We believe CIM could benefit future research on intrinsic motivation by demonstrating how attainable task priors can help design a proper intrinsic objective, and providing a general and readily applicable Lagrangian method to combine the intrinsic objective with the extrinsic objective to help find better policies whenever intrinsic bonuses are used.

A Related Work

Our work mainly belongs to maximum state entropy exploration and is related to exploration methods for sparse-reward reinforcement learning (RL).

A.1 Maximum Entropy Exploration

Maximum state entropy provable exploration has been recently proposed by Hazan [2019] to formulate the agent's intrinsic exploration behavior in the absence of the extrinsic reward signal. They argued that learning a policy to cover the state space as uniform as possible is a natural intrinsic objective for the RL agent when it cannot receive any extrinsic reward. They studied maximum state entropy in tabular MDP and state-based MuJoCo control tasks for only reward-free pure exploration. They reduced the dimension of state space by random projection and estimated the state density using kernel density estimation. Later, Mutti [2021] proposed to use nonparametric state entropy as the intrinsic objective estimated by the k-nearest neighbor (k-NN) estimator. However, they used trust-region entropy maximization and importance sampling optimization, which is not quite compatible with the state-of-the-art policy optimization algorithms like PPO and hinders further applications to challenging higher-dimensional state-based and pixel-based control tasks. To make maximum state entropy exploration more practical, Seo [2021] and Liu [2021b; 2021a] turned to define an intrinsic bonus based on k-NN estimator. Seo [2021] proposed introducing the visual inductive bias into the intrinsic bonus via the ensemble of multiple random encoders. Liu [2021b] instead proposed to learn the latent representation via a contrastive representation learning method to compute the intrinsic bonus. Liu [2021a] leveraged the successor feature technique [Hansen *et al.*, 2019] to improve the transferability of the pre-trained policy. k-NN distances were also used in other exploration researches like Tao [2020] for novelty search and Badia [2020] for directed exploration. Apart from state entropy, policy entropy [Haarnoja *et al.*, 2018], state-action entropy [Zhang *et al.*, 2021a], and relative policy entropy [Hong *et al.*, 2018; Flet-Berliac *et al.*, 2021] are also utilized to design practical exploration strategies.

A.2 Provable Exploration

Many provable exploration strategies have been developed to guarantee sublinear regret bounds or polynomial PAC bounds in various model settings, including Bandits [Auer *et al.*, 2002; Agrawal and Goyal, 2012], tabular MDP [Strehl and Littman, 2008; Osband and Van Roy, 2017; He *et al.*, 2021], linear MDP [Jin *et al.*, 2020; Zhou *et al.*, 2021; Zanette *et al.*, 2021; Wang *et al.*, 2021; Neu and Olkhovskaya, 2021; Papini *et al.*, 2021], low-rank MDP [Jiang *et al.*, 2017; Agarwal *et al.*, 2020b; Sekhari *et al.*, 2021; Zhang *et al.*, 2022], and has been recently extended into MDP with nonlinear function approximation [Feng *et al.*, 2021; Huang *et al.*, 2021]. These provable methods usually balance the exploration and exploit tradeoff by designing an intrinsic Upper Confidence Bound (UCB) exploration bonus based on the *optimism in the face of uncertainty principle* [He *et al.*, 2021; Zhang *et al.*, 2021d] or leveraging posterior sampling techniques (also known as Thompson Sampling) [Osband *et al.*, 2013; Osband and Van Roy, 2017]. However, these methods are computationally ineffective in estimating either the state density or the posterior distribution of the value function.

A.3 Practical Exploration

Practical exploration methods encourage the agent to explore novel states mainly via computationally tractable intrinsic bonuses. Pseudo-count methods extend the UCB bonus to non-tabular setting via the estimated state density [Bellemare *et al.*, 2016; Fu *et al.*, 2017]. Prediction-error-based methods use a neural network's prediction error to indicate the novelty of a state [Pathak *et al.*, 2017; Burda *et al.*, 2018]. The variance of Bayesian neural network parameters or outputs of an ensemble of neural networks is also appropriate to measure the agent's uncertainty for a state [Mavrin *et al.*, 2019; Pathak *et al.*, 2019; Lee *et al.*, 2021; Bai *et al.*, 2021b].Information gain is another approach to measuring the agent's belief about the environment [Houthooft *et al.*, 2016; Kim *et al.*, 2018; Kim *et al.*, 2019; Tao *et al.*, 2020; Bai *et al.*, 2021a]. Apart from estimating the uncertainty as novelty, some works defined the difference in consecutive states as the heuristic intrinsic bonus to stimulate the agent to explore a novel state [Marino *et al.*, 2018; Raileanu and Rocktäschel, 2020]. There are other practical approaches to tackle with the hard exploration problem, e.g., learning with auxiliary tasks [Riedmiller *et al.*, 2018], hierarchical RL [Levy *et al.*, 2017; Li *et al.*, 2019; McClinton *et al.*, 2021; Zhang *et al.*, 2021b; Gehring *et al.*, 2021], adversarially guided policy learning [Flet-Berliac *et al.*, 2021; Campero *et al.*, 2020], policy-coverage-based regularizers [Zhang *et al.*, 2021c], hindsight experience replay [Andrychowicz *et al.*, 2017; Packer *et al.*, 2021; Davchev *et al.*, 2021], memory-based policy learning [Ecoffet *et al.*, 2021; Guo *et al.*, 2020], etc.

B Environment Details

B.1 Class Control Tasks

SparseGridWorld-v0

This toy navigation task (2D state space) is adapted from the task used by MEPOL [Mutti *et al.*, 2021]. We increase the task difficulty by narrowing the wall width from 2.5m to 0.5m to increase the movement area on the map. This adjustment makes the state space larger.

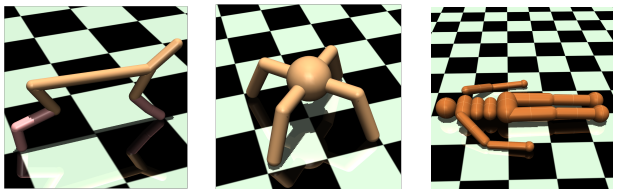

Figure 6: MuJoCo control tasks. From left to right: SparseHalfCheetah, SparseAnt, SparseHumanoidSandup

SparsePendulum-v0
This sparse-reward classic control task (3D state space) is adapted from Wulur [2021]'s work. We improve the task accuracy requirements by shrinking the angle position error threshold from 2deg to 1deg and the angular velocity error threshold from 57.3deg/s to 1deg/s. This modification makes the task extrinsic reward more sparse.

B.2 MuJoCo Control Tasks

All MuJoCo sparse-reward control tasks inherit the gym MuJoCo environments with only substitution of sparse rewards for their original hand-crafted extrinsic rewards, shown in Figure 6. The max episode steps are all 500.

SparseHalfCheetah-x20-v0
In this task, the HalfCheetah starts at $x = 0$ and learns to run forward. It can only get the extrinsic reward signal when its torso strides the plane $x = 20$. We select unit vectors of the torso position x and velocity v_x along x-axis as the base vectors of the projection space, and $m^p = [\mathbb{1}[x > 0], \mathbb{1}[v_x > 0]]$ as the masking operator.

SparseAnt-x10-v0
The Ant starts at $x = 0, y = 0$ and learns to move forward in this task. After its torso crosses the plane $x = 10$, the episode ends and it obtains an extrinsic reward signal 1. We choose unit vectors of the torso position x and velocity v_x along x-axis as the base vectors of the projection space, and $m^p = [\mathbb{1}[x > 0], \mathbb{1}[v_x > 0]]$ as the masking operator.

SparseHumanoidStandup-z1-v0
In this task, the Humanoid lies on the ground ($z \approx 0$) at the initial time and has to learn to stand up. When its torso reaches above the plane $z = 10$, it gains the nonzero extrinsic reward and the episode ends. We use unit vectors of the torso position z and velocity v_z along z-axis as the base vectors of the projection space, and $m^p = [1, \mathbb{1}[v_z > 0]]$ as the masking operator.

B.3 Discussion on Design of Task-Prior Projector

Here We discuss the details of the design principle of the task-prior projector. When the dimension of the state space is low, e.g., SGridWorld, the task-prior projector can be selected as an identity mapping, which means the projection space is the same as the full state space. When the dimension of the state space is high, we can design the task-prior projector according to the attainable high-level task information. For instance, in SparseAnt-x10-v0, the Ant is expected to run forward along x axis, thus the task-prior projector can be designed as $m^p = [\mathbb{1}[x > 0]]$ or $m^p = [\mathbb{1}[x > 0], \mathbb{1}[v_x > 0]]$. We found in our experiments that the velocity diversity is helpful for the position diversity, so we use the latter design for all experiments. One main reason we suppose is that the velocity diversity is beneficial for the agent to explore the neighborhood of the initial region in the early exploration phase. Specifically, in the early exploration phase, the agent is incapable of exploring far away from the initial region, so the bonus contributed by the position diversity is almost zero and of little help. In contrast, the agent can benefit from the velocity entropy to learn basic skills. Note that we did not search for the most appropriate task prior since our primary goal is to show how simply attainable task priors can be integrated into intrinsic motivation to benefit the agent's exploration. In fact, for the 376-D SparseHumanoidStandup-z1-v0 task, searching for the optimal projection space is intractable and unnecessary since the simple 2-D quarter projection space is sufficient enough to design a proper intrinsic objective and bonus to encourage the agent to efficiently explore only task-related regions.

Comparison with Task-agnostic Projection

Since the former maximum state entropy methods MaxEnt and MEPOL use task-agnostic projection space to tackle the high-dimension challenge, we discuss here in more detail the differences between them and our CIM to clarify further our novelty and contribution.

MaxEnt In MaxEnt, a 29-D state space of Ant is first reduced to dimension 7 by combining the agent's x and y location in the grid space with a 5-dimensional random projection of the remaining 27 states. For 376-D humanoid, they use the full state space to estimate the entropy via kernel density estimation. Therefore, as summarized in our paper's Table 1, MaxEnt uses task-agnostic projection (either random projection or the full state space) for reward-free pure exploration.

MEPOL MEPOL selects 7-D projection space (3-D spatial and 4D orientation of the torso) for Ant and 24-D projection space (3-D position, 4-D body orientation, and all joint angles) for Humanoid. These selections are all task-agnostic and aim to encourage the agent to explore all directions of the projection space in the reward-free pre-training phase.

Note that the latent space learned in APT can also be regarded as task-agnostic since the latent feature is extracted from the full state via a task-agnostic contrastive loss. By contrast, our CIM adopts the attainable task prior to constrain intrinsic motivation via the formulated task-prior projector. We demonstrate that the task-agnostic design principle for intrinsic motivation is inefficient in sparse-reward state-based continuous control tasks by comparing CIM with state-of-the-art APT on various challenging tasks.

C Implementation Details

In this section, we introduce implementation details of our CIM and all baseline intrinsic motivation methods. Source codes are included in the supplementary material.

C.1 CIM with On-policy Reinforcement Learning

CIM with on-policy RL is shown in Algorithm 1.

C.2 Default Settings

Table 2 and Table 3 shows the default configurations used for all experiments in our paper.

C.3 Baseline Implementation Details

ICM

Intrinsic Curiosity Module (ICM) [Pathak *et al.*, 2017] consists of two submodules, one is inverse dynamic predictor g which uses state features $\phi(s_t)$ and $\phi(s_{t+1})$ as input and predicts action $\hat{a}_t$, and another is forward dynamic predictor f_p which takes as input current action a_t and state feature $\phi(s_t)$ to predict the next state feature $\hat{\phi}(s_{t+1})$. The ICM loss is the summation of the two submodules' mean square error. We implement the encoder and forward and inverse dynamic predictors by three-layer Multilayer Perceptions (MLP). Note that no Batch Normalization (BN) is applied to full-connected layers in both dynamic predictors according to the implementation of ICM in URLB [Laskin *et al.*, 2020]. Only the hidden layer of the encoder applies BN. The size of the hidden layers are all `mlp_hidden_size`. The intrinsic reward of ICM is defined as the prediction error of the forward dynamic predictor f_p

$$r_t^{\text{ICM}} = \|f_p(\phi(s_t), a_t) - \phi(s_{t+1})\|.$$

RND

Random Network Distillation (RND) [Burda *et al.*, 2018] trains one neural network $f(s)$ or $f(\phi(s))$ to predict another fixed randomly initialized neural network $f^*(s)$ or $f^*(\phi(s))$ by minimizing the empirical risk and use the prediction error as the exploration bonus

$$r_t^{\text{RND}} = \|f(s_t) - f^*(s_t)\|.$$

We use the full state s as the input of RND instead of $\phi(s)$ which is usually used in pixel-based RL. The structures of $f(s)$ and $f^*(s)$ are the same as the encoder used in ICM.

MADE

Zhang [2021c] proposed a regularizer base on policy coverage that MAximizing the DEviation (MADE) of the next policy visitation from the regions covered by prior policies. It can be regarded as an amendment to RND. The MADE bonus used in the original paper is as follows

$$r_t^{\text{MADE}} = \sqrt{r_t^{\text{RND}} r_t^{\text{VAE}}}$$

where r_t^{VAE} is the prediction error of a Variational Autoencoder (VAE). We use the prediction error of an Autoencoder (AE) to estimate r_t^{VAE} in state-based RL tasks. The structure of the AE's encoder is the same as the encoder used in ICM. The AE's decoder is also a three-layer MLP of which the input is the latent state vector and the output is the full state vector. Only hidden layers of the AE's encoder and decoder apply BN.

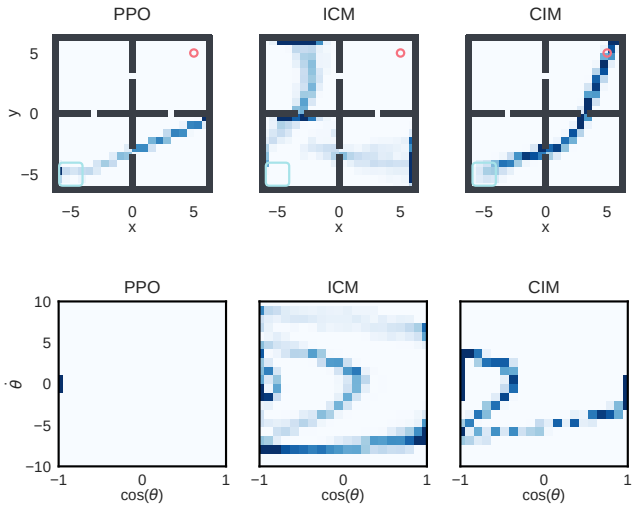

Figure 7: State Heatmaps on classic control tasks. From top to bottom: SGridWorld, SPendulum.

APT

Unsupervised Active Pre-Training (APT) uses maximum state entropy as the intrinsic objective in the reward-free pretraining phase. To scale better for high-dimensional state space, it uses the unsupervised learned latent representation of the state as the input of the k-NN nonparametric intrinsic bonus module. For pixel-based RL, it uses the contrastive loss from SimCLR [Chen *et al.*, 2020], while for state-based RL, it uses the latent state vector learned by ICM according to the implementation in URLB. We follow this implementation in our work. APT use the following reward function

$$r_t^{\text{APT}} = \ln\left(1 + \frac{1}{k}\sum_{i=1}^{k} R_{t,i}^{l/f}\right)$$

where $R_{t,i}^{l/f}$ is the i-nearest neighbour's distance from the state s_t in latent or full state space.

D Extended Analysis

In this section, we visualize the state frequency in the projection space via heatmaps to analyze the effect of the task-prior projector. We also draw the curve of the Lagrangian coefficient $\hat{\lambda}_l^{-1}$ to visualize the adaptive balance ability of the Lagrangian method.

D.1 Classic Control Tasks

From Figure 7, we can clearly see that only our CIM can explore sufficiently and cover the target state, i.e., (5,5) in SGridWorld and (1,0) in SPendulum. Specifically, in SGridWorld, oracle PPO without any intrinsic motivation can only accidentally go through a door with a simple straight trajectory. Though ICM has a better state coverage behavior than oracle PPO, it struggles in the neighbor room and cannot reach the target room. Our CIM has the best exploration behavior. What's more, once the agent is capable of obtaining the sparse extrinsic reward, the inverse Lagrangian coefficient

Algorithm 1: CIM with On-policy RL

Initialize the policy π_θ, extrinsic value function V_{ϕ^e}, and intrinsic value function V_{ϕ^i}
Initialize the replay buffer $\mathcal{B}$ and the step counter $t = 0$
Initialize the Lagrangian coefficent $\lambda_0 = 1$, the expected reward $\hat{R}_0 = 0$ and the batch counter $l = 0$
while $t < T$ **do**
  `// Collect samples`
  Collector a batch of samples $\mathcal{D} = \{(s_t, a_t, r_t^e, s_{t+1})\}$ using the policy π_{θ_l}
  Update $\mathcal{B}$ with $\mathcal{D}$ via FIFO
  $t = t + \text{len}(\mathcal{D})$
  `// Compute intrinsic reward using samples in` $\mathcal{B}$
  Compute the $i-$nearest distance $R_{t,i}^p$ for all $\text{proj}_\mathcal{P}\ s_t$ in projection space $\mathcal{P}$
  Compute CIM bonus $r_t^{\text{CIM}} = \ln\left(1 + \frac{1}{k}\sum_{i=1}^{k} R_{t,i}^p\right)$
  `// Compute intrinsic reward coefficient using samples in` $\mathcal{D}$
  Update the Lagrangian coefficient $\lambda_{l+1} = \lambda_l - \eta_l(f_e(d_{\pi_l}) - \hat{R}_l)$
  Update the expected reward $\hat{R}_{l+1} = \alpha f_e(d_{\pi_l})$
  $l = l + 1$
  `// Compute advantages using samples in` $\mathcal{D}$
  Compute advantage $A^e(s_t, a_t)$ and return $R^e(s_t)$ based on $\{r_t^e\}$ via Generalized Advantage Estimator (GAE)
  Compute advantage $A^i(s_t, a_t)$ and return $R^i(s_t)$ based on $\{r_t^{\text{CIM}}\}$ via GAE
  `// Update the policy and critics`
  Compute total advantage $A(s_t, a_t) = \lambda_l^{-1} A^i(s_t, a_t) + A^e(s_t, a_t)$
  $loss_\theta = \sum_{s\sim\mathcal{D}} \min\left\{\frac{\pi^\theta(a|s)}{\pi^{\theta_l}(a|s)} A(s,a), \text{clip}\left(\frac{\pi^\theta(a|s)}{\pi^{\theta_l}(a|s)}; 1-\epsilon, 1+\epsilon\right) A(s,a)\right\}$
  $loss_{\phi^e} = \sum_{s\sim\mathcal{D}} \left(V_{\phi^e}(s) - R^e(s)\right)^2$
  $loss_{\phi^i} = \sum_{s\sim\mathcal{D}} \left(V_{\phi^i}(s) - R^i(s)\right)^2$
  Gradient descent step on θ, ϕ^e, and ϕ^i
end

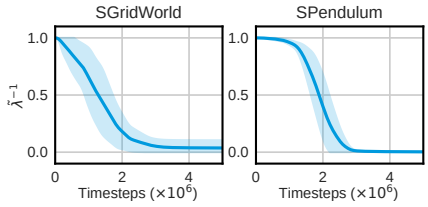

Figure 8: The Lagrangian coefficient curves on classic control tasks.

starts to decrease to reduce the strength of the intrinsic motivation, as shown in Figure 8. A similar phenomenon can also be observed in SPendulum.

D.2 MuJoCo Control Tasks

Figure 9 clearly shows the effect of the task-prior projector. Our novel task-prior projector effectively constrains the agent to explore only the quarter projection space. Once the agent is able to cross the target line to get the sparse extrinsic reward, the Lagrangian method takes effect and the inverse Lagrangian coefficient gradually decreases to zero to reduce the bias introduced by the intrinsic motivation. Although ICM can encourage the agent to explore further than oracle PPO, the agent takes useless effort to explore all directions in the projection space without being constrained by the attainable task prior.

E Extended Ablation Study

We do an extended ablation study on the parameter of the k-nearest neighbor (k-NN) entropy estimator. As shown in Figure 11, the estimator is insensitive to the parameter k. $k = 10$ is reasonably consistent across high-dimensional tasks.

Table 2: Default collector settings used in experiments.

Parameter Name	Default value	Comments
total_timesteps	5e6	
max_epoch	20	only affect test frequency
step_per_collect	1024 * 8	a.k.a batch_size
n_minibatch	4	
n_env	8 * 8	
test_num	8	
episode_per_test	8	
repeat_per_collect	10	times the batch is repeated

Table 3: Default policy settings used in experiments.

Parameter Name	Default value	Comments
reward_normalization	True	
discount_factor	0.99	
gae_lambda	0.95	
max_grad_norm	0.5	
eps_clip ϵ	0.2	
advantage_normalization	True	
recompute_advantage	False	
action_bound_method	”clip”	in [”clip”, ”tanh”, ”none”]
action_scaling_bool	True	
deterministic_eval	True	
cache_size	int(1e6)	
sa_ent	False	
k	10	
training_paradigm	MISSING	in [”NI”, ”RF”, ”P”, ”L”]
proj	False	
space	”full”	in [”full”, ”p_v”, ”p”]
masking	False	
reward_free_ratio	0.5	
expect_reward_coefficient α	2	
Lagrangian_step_size η	1	
hidden_sizes	[64,64]	of policy network and value networks
init_logsigma	log(1)	
learning_rate	3e-4	
mlp_hidden_dim	128	of MLPs used for the encoder and intrinsic modules
obs_rep_dim	64	dimension of latent state
mlp_norm	”BN”	normalization techniques applied to MLPs

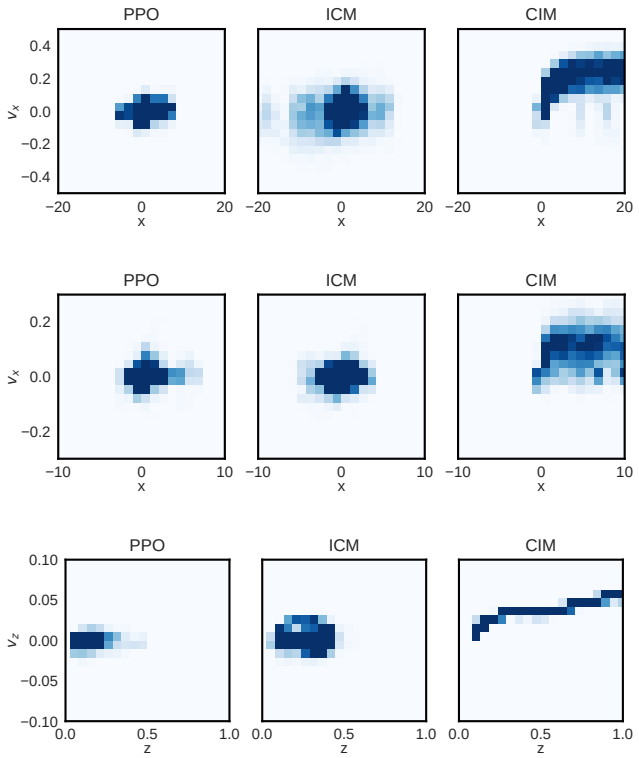

Figure 9: State Heatmaps on MuJoCo control tasks. From top to bottom: SparseHalfCheetah, SparseAnt, SparseHumanoidSandup

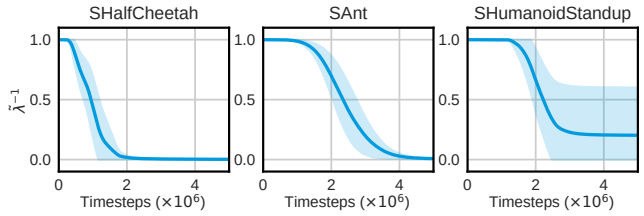

Figure 10: The Lagrangian coefficient curves on MuJoCo control tasks.

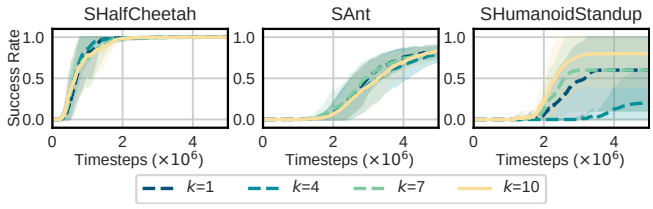

Figure 11: Ablation Study on MuJoCo control tasks.

References

[Agarwal *et al.*, 2020a] Alekh Agarwal, Mikael Henaff, Sham Kakade, and Wen Sun. Pc-pg: Policy cover directed exploration for provable policy gradient learning. *Advances in neural information processing systems*, 33:13399–13412, 2020.

[Agarwal *et al.*, 2020b] Alekh Agarwal, Sham Kakade, Akshay Krishnamurthy, and Wen Sun. Flambe: Structural complexity and representation learning of low rank mdps. *Advances in neural information processing systems*, 33:20095–20107, 2020.

[Agrawal and Goyal, 2012] Shipra Agrawal and Navin Goyal. Analysis of thompson sampling for the multi-armed bandit problem. In *Conference on learning theory*, pages 39–1. JMLR Workshop and Conference Proceedings, 2012.

[Andrychowicz *et al.*, 2017] Marcin Andrychowicz, Filip Wolski, Alex Ray, Jonas Schneider, Rachel Fong, Peter Welinder, Bob McGrew, Josh Tobin, OpenAI Pieter Abbeel, and Wojciech Zaremba. Hindsight experience replay. *Advances in neural information processing systems*, 30, 2017.

[Auer *et al.*, 2002] Peter Auer, Nicolo Cesa-Bianchi, and Paul Fischer. Finite-time analysis of the multiarmed bandit problem. *Machine learning*, 47(2):235–256, 2002.

[Badia *et al.*, 2020] Adrià Puigdomènech Badia, Pablo Sprechmann, Alex Vitvitskyi, Daniel Guo, Bilal Piot, Steven Kapturowski, Olivier Tieleman, Martín Arjovsky, Alexander Pritzel, Andew Bolt, et al. Never give up: Learning directed exploration strategies. *arXiv preprint arXiv:2002.06038*, 2020.

[Bai *et al.*, 2021a] Chenjia Bai, Lingxiao Wang, Lei Han, Animesh Garg, Jianye Hao, Peng Liu, and Zhaoran Wang. Dynamic bottleneck for robust self-supervised exploration. *Advances in Neural Information Processing Systems*, 34:17007–17020, 2021.

[Bai *et al.*, 2021b] Chenjia Bai, Lingxiao Wang, Lei Han, Jianye Hao, Animesh Garg, Peng Liu, and Zhaoran Wang. Principled exploration via optimistic bootstrapping and backward induction. In *International Conference on Machine Learning*, pages 577–587. PMLR, 2021.

[Barto, 2013] Andrew G Barto. Intrinsic motivation and reinforcement learning. In *Intrinsically motivated learning in natural and artificial systems*, pages 17–47. Springer, 2013.

[Bellemare *et al.*, 2016] Marc Bellemare, Sriram Srinivasan, Georg Ostrovski, Tom Schaul, David Saxton, and Remi Munos. Unifying count-based exploration and intrinsic motivation. *Advances in neural information processing systems*, 29, 2016.

[Burda *et al.*, 2018] Yuri Burda, Harrison Edwards, Amos Storkey, and Oleg Klimov. Exploration by random network distillation. *arXiv preprint arXiv:1810.12894*, 2018.

[Campero *et al.*, 2020] Andres Campero, Roberta Raileanu, Heinrich Küttler, Joshua B Tenenbaum, Tim Rocktäschel, and Edward Grefenstette. Learning with amigo: Adversarially motivated intrinsic goals. *arXiv preprint arXiv:2006.12122*, 2020.

[Cesa-Bianchi *et al.*, 2017] Nicolò Cesa-Bianchi, Claudio Gentile, Gábor Lugosi, and Gergely Neu. Boltzmann exploration done right. *Advances in neural information processing systems*, 30, 2017.

[Chen *et al.*, 2020] Ting Chen, Simon Kornblith, Mohammad Norouzi, and Geoffrey Hinton. A simple framework for contrastive learning of visual representations. In *International conference on machine learning*, pages 1597–1607. PMLR, 2020.

[Davchev *et al.*, 2021] Todor Davchev, Oleg Sushkov, Jean-Baptiste Regli, Stefan Schaal, Yusuf Aytar, Markus Wulfmeier, and Jon Scholz. Wish you were here: Hindsight goal selection for long-horizon dexterous manipulation. *arXiv preprint arXiv:2112.00597*, 2021.

[Ecoffet *et al.*, 2021] Adrien Ecoffet, Joost Huizinga, Joel Lehman, Kenneth O Stanley, and Jeff Clune. First return, then explore. *Nature*, 590(7847):580–586, 2021.

[Feng *et al.*, 2021] Fei Feng, Wotao Yin, Alekh Agarwal, and Lin Yang. Provably correct optimization and exploration with non-linear policies. In *International Conference on Machine Learning*, pages 3263–3273. PMLR, 2021.

[Feydy *et al.*, 2020] Jean Feydy, Alexis Glaunès, Benjamin Charlier, and Michael Bronstein. Fast geometric learning with symbolic matrices. *Advances in Neural Information Processing Systems*, 33:14448–14462, 2020.

[Flet-Berliac *et al.*, 2021] Yannis Flet-Berliac, Johan Ferret, Olivier Pietquin, Philippe Preux, and Matthieu Geist. Adversarially guided actor-critic. *arXiv preprint arXiv:2102.04376*, 2021.

[Fu *et al.*, 2017] Justin Fu, John Co-Reyes, and Sergey Levine. Ex2: Exploration with exemplar models for deep reinforcement learning. *Advances in neural information processing systems*, 30, 2017.

[Gehring *et al.*, 2021] Jonas Gehring, Gabriel Synnaeve, Andreas Krause, and Nicolas Usunier. Hierarchical skills for efficient exploration. *Advances in Neural Information Processing Systems*, 34:11553–11564, 2021.

[Guo *et al.*, 2020] Yijie Guo, Jongwook Choi, Marcin Moczulski, Shengyu Feng, Samy Bengio, Mohammad Norouzi, and Honglak Lee. Memory based trajectory-conditioned policies for learning from sparse rewards. *Advances in Neural Information Processing Systems*, 33:4333–4345, 2020.

[Haarnoja *et al.*, 2018] Tuomas Haarnoja, Aurick Zhou, Kristian Hartikainen, George Tucker, Sehoon Ha, Jie Tan, Vikash Kumar, Henry Zhu, Abhishek Gupta, Pieter Abbeel, et al. Soft actor-critic algorithms and applications. *arXiv preprint arXiv:1812.05905*, 2018.

[Hansen *et al.*, 2019] Steven Hansen, Will Dabney, Andre Barreto, Tom Van de Wiele, David Warde-Farley,

and Volodymyr Mnih. Fast task inference with variational intrinsic successor features. *arXiv preprint arXiv:1906.05030*, 2019.

[Hazan *et al.*, 2019] Elad Hazan, Sham Kakade, Karan Singh, and Abby Van Soest. Provably efficient maximum entropy exploration. In *International Conference on Machine Learning*, pages 2681–2691. PMLR, 2019.

[He *et al.*, 2021] Jiafan He, Dongruo Zhou, and Quanquan Gu. Nearly minimax optimal reinforcement learning for discounted mdps. *Advances in Neural Information Processing Systems*, 34:22288–22300, 2021.

[Hong *et al.*, 2018] Zhang-Wei Hong, Tzu-Yun Shann, Shih-Yang Su, Yi-Hsiang Chang, Tsu-Jui Fu, and Chun-Yi Lee. Diversity-driven exploration strategy for deep reinforcement learning. *Advances in neural information processing systems*, 31, 2018.

[Houthooft *et al.*, 2016] Rein Houthooft, Xi Chen, Yan Duan, John Schulman, Filip De Turck, and Pieter Abbeel. Vime: Variational information maximizing exploration. *Advances in neural information processing systems*, 29, 2016.

[Huang *et al.*, 2021] Baihe Huang, Kaixuan Huang, Sham Kakade, Jason D Lee, Qi Lei, Runzhe Wang, and Jiaqi Yang. Going beyond linear rl: Sample efficient neural function approximation. *Advances in Neural Information Processing Systems*, 34:8968–8983, 2021.

[Jiang *et al.*, 2017] Nan Jiang, Akshay Krishnamurthy, Alekh Agarwal, John Langford, and Robert E Schapire. Contextual decision processes with low bellman rank are pac-learnable. In *International Conference on Machine Learning*, pages 1704–1713. PMLR, 2017.

[Jiao *et al.*, 2018] Jiantao Jiao, Weihao Gao, and Yanjun Han. The nearest neighbor information estimator is adaptively near minimax rate-optimal. *Advances in neural information processing systems*, 31, 2018.

[Jin *et al.*, 2020] Chi Jin, Zhuoran Yang, Zhaoran Wang, and Michael I Jordan. Provably efficient reinforcement learning with linear function approximation. In *Conference on Learning Theory*, pages 2137–2143. PMLR, 2020.

[Kim *et al.*, 2018] Hyoungseok Kim, Jaekyeom Kim, Yeonwoo Jeong, Sergey Levine, and Hyun Oh Song. Emi: Exploration with mutual information. *arXiv preprint arXiv:1810.01176*, 2018.

[Kim *et al.*, 2019] Youngjin Kim, Wontae Nam, Hyunwoo Kim, Ji-Hoon Kim, and Gunhee Kim. Curiosity-bottleneck: Exploration by distilling task-specific novelty. In *International Conference on Machine Learning*, pages 3379–3388. PMLR, 2019.

[Laskin *et al.*, 2020] Michael Laskin, Aravind Srinivas, and Pieter Abbeel. Curl: Contrastive unsupervised representations for reinforcement learning. In *International Conference on Machine Learning*, pages 5639–5650. PMLR, 2020.

[Laskin *et al.*, 2021] Michael Laskin, Denis Yarats, Hao Liu, Kimin Lee, Albert Zhan, Kevin Lu, Catherine Cang, Lerrel Pinto, and Pieter Abbeel. Urlb: Unsupervised reinforcement learning benchmark. *arXiv preprint arXiv:2110.15191*, 2021.

[Lee *et al.*, 2021] Kimin Lee, Michael Laskin, Aravind Srinivas, and Pieter Abbeel. Sunrise: A simple unified framework for ensemble learning in deep reinforcement learning. In *International Conference on Machine Learning*, pages 6131–6141. PMLR, 2021.

[Levy *et al.*, 2017] Andrew Levy, George Konidaris, Robert Platt, and Kate Saenko. Learning multi-level hierarchies with hindsight. *arXiv preprint arXiv:1712.00948*, 2017.

[Li *et al.*, 2019] Alexander C Li, Carlos Florensa, Ignasi Clavera, and Pieter Abbeel. Sub-policy adaptation for hierarchical reinforcement learning. *arXiv preprint arXiv:1906.05862*, 2019.

[Liu and Abbeel, 2021a] Hao Liu and Pieter Abbeel. Aps: Active pretraining with successor features. In *International Conference on Machine Learning*, pages 6736–6747. PMLR, 2021.

[Liu and Abbeel, 2021b] Hao Liu and Pieter Abbeel. Behavior from the void: Unsupervised active pre-training. *Advances in Neural Information Processing Systems*, 34:18459–18473, 2021.

[Marino *et al.*, 2018] Kenneth Marino, Abhinav Gupta, Rob Fergus, and Arthur Szlam. Hierarchical rl using an ensemble of proprioceptive periodic policies. In *International Conference on Learning Representations*, 2018.

[Mavrin *et al.*, 2019] Borislav Mavrin, Hengshuai Yao, Linglong Kong, Kaiwen Wu, and Yaoliang Yu. Distributional reinforcement learning for efficient exploration. In *International conference on machine learning*, pages 4424–4434. PMLR, 2019.

[McClinton *et al.*, 2021] Willie McClinton, Andrew Levy, and George Konidaris. Hac explore: Accelerating exploration with hierarchical reinforcement learning. *arXiv preprint arXiv:2108.05872*, 2021.

[Mutti *et al.*, 2021] Mirco Mutti, Lorenzo Pratissoli, and Marcello Restelli. Task-agnostic exploration via policy gradient of a non-parametric state entropy estimate. In *Proceedings of the AAAI Conference on Artificial Intelligence*, volume 35, pages 9028–9036, 2021.

[Neu and Olkhovskaya, 2021] Gergely Neu and Julia Olkhovskaya. Online learning in mdps with linear function approximation and bandit feedback. *Advances in Neural Information Processing Systems*, 34:10407–10417, 2021.

[Osband and Van Roy, 2017] Ian Osband and Benjamin Van Roy. Why is posterior sampling better than optimism for reinforcement learning? In *International conference on machine learning*, pages 2701–2710. PMLR, 2017.

[Osband *et al.*, 2013] Ian Osband, Daniel Russo, and Benjamin Van Roy. (more) efficient reinforcement learning via posterior sampling. *Advances in Neural Information Processing Systems*, 26, 2013.

[Packer *et al.*, 2021] Charles Packer, Pieter Abbeel, and Joseph E Gonzalez. Hindsight task relabelling: Experience replay for sparse reward meta-rl. *Advances in Neural Information Processing Systems*, 34:2466–2477, 2021.

[Papini *et al.*, 2021] Matteo Papini, Andrea Tirinzoni, Aldo Pacchiano, Marcello Restelli, Alessandro Lazaric, and Matteo Pirotta. Reinforcement learning in linear mdps: Constant regret and representation selection. *Advances in Neural Information Processing Systems*, 34:16371–16383, 2021.

[Pathak *et al.*, 2017] Deepak Pathak, Pulkit Agrawal, Alexei A Efros, and Trevor Darrell. Curiosity-driven exploration by self-supervised prediction. In *International conference on machine learning*, pages 2778–2787. PMLR, 2017.

[Pathak *et al.*, 2019] Deepak Pathak, Dhiraj Gandhi, and Abhinav Gupta. Self-supervised exploration via disagreement. In *International conference on machine learning*, pages 5062–5071. PMLR, 2019.

[Plappert *et al.*, 2017] Matthias Plappert, Rein Houthooft, Prafulla Dhariwal, Szymon Sidor, Richard Y Chen, Xi Chen, Tamim Asfour, Pieter Abbeel, and Marcin Andrychowicz. Parameter space noise for exploration. *arXiv preprint arXiv:1706.01905*, 2017.

[Puterman, 2014] Martin L Puterman. *Markov decision processes: discrete stochastic dynamic programming*. John Wiley & Sons, 2014.

[Raileanu and Rocktäschel, 2020] Roberta Raileanu and Tim Rocktäschel. Ride: Rewarding impact-driven exploration for procedurally-generated environments. *arXiv preprint arXiv:2002.12292*, 2020.

[Riedmiller *et al.*, 2018] Martin Riedmiller, Roland Hafner, Thomas Lampe, Michael Neunert, Jonas Degrave, Tom Wiele, Vlad Mnih, Nicolas Heess, and Jost Tobias Springenberg. Learning by playing solving sparse reward tasks from scratch. In *International conference on machine learning*, pages 4344–4353. PMLR, 2018.

[Schulman *et al.*, 2017] John Schulman, Filip Wolski, Prafulla Dhariwal, Alec Radford, and Oleg Klimov. Proximal policy optimization algorithms. *arXiv preprint arXiv:1707.06347*, 2017.

[Sekhari *et al.*, 2021] Ayush Sekhari, Christoph Dann, Mehryar Mohri, Yishay Mansour, and Karthik Sridharan. Agnostic reinforcement learning with low-rank mdps and rich observations. *Advances in Neural Information Processing Systems*, 34:19033–19045, 2021.

[Seo *et al.*, 2021] Younggyo Seo, Lili Chen, Jinwoo Shin, Honglak Lee, Pieter Abbeel, and Kimin Lee. State entropy maximization with random encoders for efficient exploration. In *International Conference on Machine Learning*, pages 9443–9454. PMLR, 2021.

[Sharma *et al.*, 2019] Archit Sharma, Shixiang Gu, Sergey Levine, Vikash Kumar, and Karol Hausman. Dynamics-aware unsupervised discovery of skills. *arXiv preprint arXiv:1907.01657*, 2019.

[Strehl and Littman, 2008] Alexander L Strehl and Michael L Littman. An analysis of model-based interval estimation for markov decision processes. *Journal of Computer and System Sciences*, 74(8):1309–1331, 2008.

[Tao *et al.*, 2020] Ruo Yu Tao, Vincent François-Lavet, and Joelle Pineau. Novelty search in representational space for sample efficient exploration. *Advances in Neural Information Processing Systems*, 33:8114–8126, 2020.

[Wang *et al.*, 2021] Tianhao Wang, Dongruo Zhou, and Quanquan Gu. Provably efficient reinforcement learning with linear function approximation under adaptivity constraints. *Advances in Neural Information Processing Systems*, 34:13524–13536, 2021.

[Weng *et al.*, 2021] Jiayi Weng, Huayu Chen, Dong Yan, Kaichao You, Alexis Duburcq, Minghao Zhang, Hang Su, and Jun Zhu. Tianshou: A highly modularized deep reinforcement learning library. *arXiv preprint arXiv:2107.14171*, 2021.

[Wulur *et al.*, 2021] Christoper Wulur, Cornelius Weber, and Stefan Wermter. Planning-integrated policy for efficient reinforcement learning in sparse-reward environments. In *2021 International Joint Conference on Neural Networks (IJCNN)*, pages 1–8. IEEE, 2021.

[Zanette *et al.*, 2021] Andrea Zanette, Ching-An Cheng, and Alekh Agarwal. Cautiously optimistic policy optimization and exploration with linear function approximation. In *Conference on Learning Theory*, pages 4473–4525. PMLR, 2021.

[Zhang *et al.*, 2021a] Chuheng Zhang, Yuanying Cai, Longbo Huang, and Jian Li. Exploration by maximizing rényi entropy for reward-free rl framework. In *Proceedings of the AAAI Conference on Artificial Intelligence*, volume 35, pages 10859–10867, 2021.

[Zhang *et al.*, 2021b] Jesse Zhang, Haonan Yu, and Wei Xu. Hierarchical reinforcement learning by discovering intrinsic options. *arXiv preprint arXiv:2101.06521*, 2021.

[Zhang *et al.*, 2021c] Tianjun Zhang, Paria Rashidinejad, Jiantao Jiao, Yuandong Tian, Joseph E Gonzalez, and Stuart Russell. Made: Exploration via maximizing deviation from explored regions. *Advances in Neural Information Processing Systems*, 34:9663–9680, 2021.

[Zhang *et al.*, 2021d] Zihan Zhang, Yuan Zhou, and Xiangyang Ji. Model-free reinforcement learning: from clipped pseudo-regret to sample complexity. In *International Conference on Machine Learning*, pages 12653–12662. PMLR, 2021.

[Zhang *et al.*, 2022] Xuezhou Zhang, Yuda Song, Masatoshi Uehara, Mengdi Wang, Alekh Agarwal, and Wen Sun. Efficient reinforcement learning in block mdps: A model-free representation learning approach. In *International Conference on Machine Learning*, pages 26517–26547. PMLR, 2022.

[Zhou *et al.*, 2021] Dongruo Zhou, Quanquan Gu, and Csaba Szepesvari. Nearly minimax optimal reinforcement learn-

ing for linear mixture markov decision processes. In *Conference on Learning Theory*, pages 4532–4576. PMLR, 2021.